Finite element modeling of a two-fluid RF plasma discharge

Haribalan Kumar, Subrata Roy*

Computational Plasma Dynamics Laboratory, Kettering University, Flint, Michigan 48504, USA

Abstract

The design and understanding of plasma and its bounding sheath requires an effective modeling technique that is both adaptable to arbitrary geometry and time accurate. We present a finite-element-based model for two-fluid plasma. The continuity and momentum equations for electrons and ions are solved simultaneously with the Poisson equation, using an efficient subgrid-embedded algorithm. The model does not involve any conventional patching techniques at the plasma–sheath interface. The solutions are interpreted using the speed of ionization as one key parameter determining collisional sheath behavior. Numerical limitations are also analyzed from the theoretical derivation of solution amplification factor and phase velocity.

Keywords: RF discharge; Sheath; Phase velocity; Finite element; Ionization

1. Introduction

There have been a number of attempts to model the dynamics of plasma and sheath, such as those by Godyak and Sternberg [1], Nitschke and Graves [2], Boeuf and Pitchford [3], and Roy et al. [4]. A part of the literature on the plasma–sheath modeling suggests that this transition can be modeled separately by matching step–sheath model and bulk-plasma model [1]. However, it is not clear how properly to match the sheath to the bulk plasma for a time dependent sheath [2]. Hence we focus on simulation of radio frequency (RF) interactions with fluids from first-principles. A combined plasma-wall model is appropriate where the space charge effect is incorporated for the entire region [3]. Recently, a one-dimensional formulation of the same has been reported [4]. While the model describes the RF system, the detailed results for number densities and currents are not documented. Here we report the details of the simulation results for a RF-based discharge in low pressure regime with its bounding collisional sheath.

2. The plasma wall problem

The solution of plasma extending from the bulk up to and including the wall is modeled here using one-dimensional hydrodynamic equations for electron and ion, coupled with the Poisson equation for potential.

2.1 Model

The continuity and momentum equations are given by [3,4]

$$\frac{\partial n_a}{\partial t}+\frac{\partial(n_aV_a)}{\partial x}=n_e z \quad \text{for} \quad \alpha=e,i \quad \text{with} \quad n_aV_a=\pm n_a\mu_aE-D_a\frac{\partial n_a}{\partial x} \tag{1}$$

The ionization rate for argon gas is given by $z = Ae^{-B/(E/p)^{0.4}}\, p\Re$. We introduce $\Re$ (with dimension m/s) as the 'speed of ionization' to model the spatially and temporally varying ionization where $\Re = \mu_e E$ as given by the 'modified' ionization equation. The following Poisson equation is used to calculate the potential drop across the working gas argon of dielectric constant ϵ (with a relative permittivity $\approx$1.0055):

$$\varepsilon\frac{\partial^2\varphi}{\partial x^2}=e(n_e-n_i) \tag{2}$$

where e is the elementary charge. The electrons are at a temperature of $T_e = 1\,\text{eV}$ (11,600 K) and the ions are assumed cold at 300 K. The electrode at $x=0$ is grounded, while a time-varying potential $\varphi_{rf} = \varphi_{rms} \sin 2\pi ft$ with $\varphi_{rms}=100\text{V}$ and $f=13.56\,\text{MHz}$ is applied at $x = 2\,\text{cm}$. The gas pressure is 0.1 Torr.

* Corresponding author. Tel.: + 810–762–9949; Fax: + 810–762–7985; E-mail: Sroy@kettering.edu

Computational Fluid and Solid Mechanics 2005
K.J. Bathe (Editor) **Paper no. 226-333**

2.2 Boundary conditions

The problem is considered in its entirety without imposing any conditions at plasma edge for solving the bounding sheath. The sheath edge is identified and $V_i/V_B = [1 + \alpha]^{-0.5}$ is the ion sonic for the collision parameter $\alpha = 0.5\pi\lambda_D/\lambda_i$ where λ_D is the Debye length, the effective ion mean free path λ_i(cm) $\sim$1/330P (in torr), and V_B is the ion sonic (Bohm) velocity.

The electron flux at the electrodes is based on the thermalized electron velocity whose magnitude is given by $I_e = n_e V_{e,\text{th}}$. Homogeneous Neumann boundary condition ($\partial n_i/\partial_z = 0$) is applied for ions at electrodes. For the Poisson equation we used $\varphi(0) = 0$ and $\varphi(2) = \varphi_c$ where φ_c is calculated from the following current balance

$$I_{tot}(t) = \varepsilon\frac{\partial E}{\partial t} + en_i V_i - en_e V_e \tag{3}$$

The equations (1)–(3) are normalized using the following dimensionless quantities, $\tau = 2\pi ft$, $z = x/d$, $S = zd/V_B$, $N_\alpha = n_\alpha/n_0$, $u_\alpha = V_\alpha/V_B$ and $\phi = e\varphi/T_e$ where d is inter-electrode length.

3. Numerical methodology

We utilized multiscale ionized gas (MIG) flow code anchored in a powerful high-fidelity finite-element procedure that has been benchmarked and validated against a range of plasma wall problems [5,6]. Here the methodology is adopted to overcome the stiffness of the above system of equations, Eqs. (1)–(3).

3.1 Galerkin weak statement (GWS)

For the stated RF bounded plasma discharge, the equation set can be written with operator L, as $\mathrm{L}(\mathbf{q}) = 0$ where $\mathbf{q} = \{\mathrm{N_i}, \mathrm{N_e}, \phi\}^{\mathrm{T}}$. Multiplying with a permissible test function Ψ and integrating over the spatially discretized solution domain Ω, the variational statement results in the weak form $WS^h = \mathrm{S_e}\left(\int_{\Omega_e}[\Psi L(\boldsymbol{q})d\tau]\right)_{\mathrm{e}} = 0$ for a discretization h of domain $\Omega = \cup\Omega_e$ and S_e is the non-overlapping sum over the elements. Thus the GWS form of Eq. (1) becomes

$$S_e\left(\int_{\Omega_e}\Psi\Psi^T dx\left(\frac{d\{N_\alpha\}_e}{dt}\right) + \left\{\int_{\partial\Omega_e}\Psi(\Gamma_\alpha)^T dx\{N_\alpha\}_e - \int_{\Omega_e}\frac{d\Psi}{dx}(\Gamma_\alpha)^T dx\{N_\alpha\}_e\right\} - \int_{\Omega_e}\Psi\Psi^T dx\{N_e\}_e)_e = F_\alpha \tag{4}$$

where F_α is the solution residual, and the GWS form of Eq. (2) with residual F_ϕ is

$$S_e\left(-\int_{\partial\Omega_e}\Psi\frac{d\Psi^T}{dx}dx\{\phi\}_e + \int_{\Omega_e}\frac{d\Psi}{dx}\frac{d\Psi^T}{dx}dx\{\phi\}_e + \int_{\Omega_e}\Psi\Psi^T dx\{N_e\}_e - \int_{\Omega_e}\Psi\Psi^T dx\{N_i\}_e)_e = F_\phi \tag{5}$$

The terminal non-linear ordinary differential equation (ODE) systems derived from Eqs. (4)–(5) are solved using implicit Euler method and N-R iterative algorithm. The domain is discretized into 200 elements and ψ is interpolated using a linear basis function. The Jacobian matrix $J = [\partial F/\partial Q]$ in $[J].\{\partial Q\} = -\{F\}$ is resolved using LU-decomposition scheme for updating change in discretized solution vector Q at each iteration. The convergence criterion for all variables at any iteration is 10^{-3}.

3.2 Amplification factor and phase velocity

The stability of the above algorithm in section 3.1 can be investigated from the solution amplification factor G^h, its magnitude $|G^h|$ and the relative phase velocity Φ^h. For example, based on the finite element stencil for Eq. (4) one may derive the following factors for ions:

$$G^h = [1 - 3iCf(\omega\Delta x) - S\Delta t(\cos\theta + i\sin\theta)]^{-1} \tag{6}$$

$$|G^h| = \left((1 - S\Delta t\cos\theta)^2 + (3Cf(\omega\Delta x) + S\Delta t\sin\theta)^2\right)^{-0.5}$$

$$\Phi^h = \tan^{-1}\left[\frac{(3Cf(\omega\Delta x) + S\Delta t\sin\theta)}{(1 - S\Delta t\cos\theta)}\right]\Big/ -C\omega\Delta x \tag{7}$$

while those for electrons are:

$$G^h = [1 - 3iCf(\omega\Delta x) - S\Delta t]^{-1}, \quad |G^h| = [(1 - S\Delta t)^2 + (3Cf(\omega\Delta x))^2 \tag{8}$$

$$\Phi^h = \tan^{-1}\left[\frac{3Cf(\omega\Delta x)}{(1 - S\Delta t)}\right]\Big/ -C\omega\Delta x \tag{9}$$

where ω is the wave number, Δx is the length of an element, C is the Courant number, $f(\omega\Delta x) = \sin\omega\Delta x/(2 + \cos\omega\Delta x)$ and $\theta = -(u_e^h - u_i^h)\omega(\mathrm{n} + 1)\Delta\mathrm{t}$ is the relative velocity phase angle.

The algorithm is stable if $|G^h| \leq 1$. One prefers $\Phi^h \sim 1$ to minimize the loss of information during solution process. Figure 1 plots $|G^h|$ and Φ^h as functions of $\omega\Delta x$ and C for $\theta = 0$ (hence true for both ions and electrons). Obviously, for the higher value of ionization rate S2 = 500, the solution becomes unstable. The numerical difficulty may be handled by the appropriate selection of Courant number and the introduction of artificial

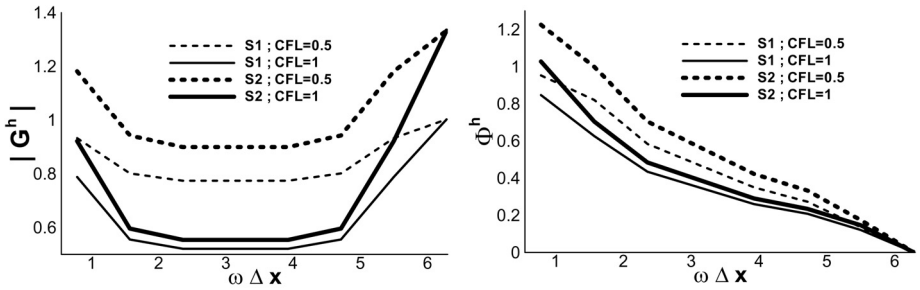

Fig. 1. Amplification factor ($|G^h|$) and relative phase velocity (Φ^h) for different Courant numbers (CFL), and ionization rates S1 = 5 and S2 = 500.

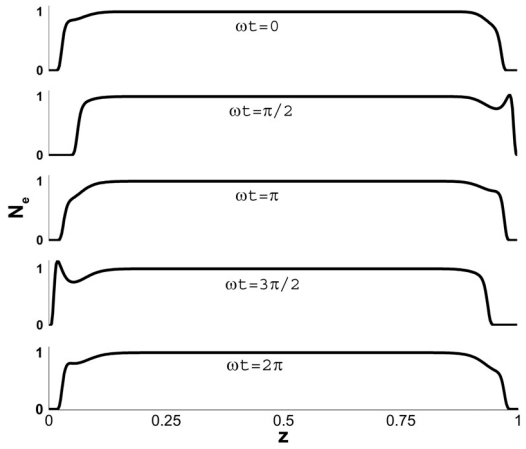

Fig. 2. Temporal evolution of normalized electron number density (N_e).

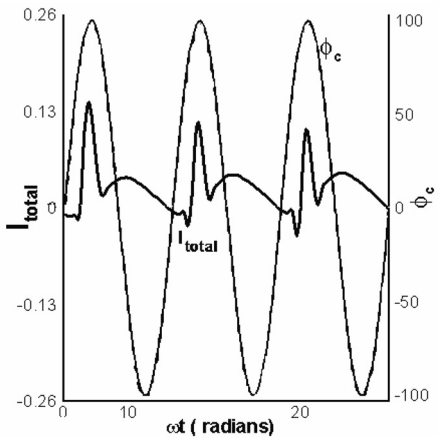

Fig. 3. Periodic nature of the potential and normalized total current at the powered electrode.

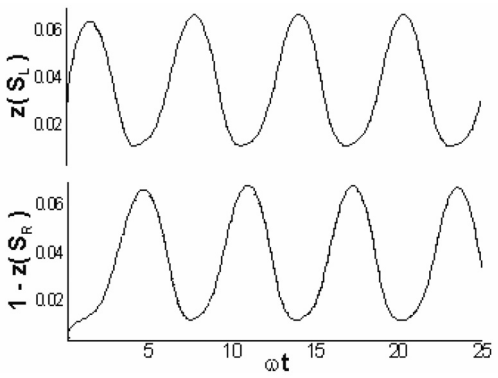

Fig. 4. Temporal oscillation of left (S_L) and right (1-S_R) normalized sheath width.

diffusion. Interestingly, any further increase of S (> 500) brings the system back to stability (not shown in the fig.). This demonstrates a nice balance between $S\Delta t$ and Cf ($\omega\Delta x$) that will be elaborated in an ensuing paper.

4. Results and discussions

Figures 2–4 describe the computed solution using the methodology stated above. The momentary rise of the electron wave at the alternate electrodes in Fig. 2 at every $\pi/2$ and $3\pi/2$ radians shows a typical RF characteristic. For most of the remaining time, the charge-separated sheath region is mostly devoid of electrons. Fig. 3 shows the variation of total current as given by Eq. (3) with the computed potential. The periodicity of the peak total current is observed near ($\pi/2$ + 2pπ) radian; p $\geq$ 0 is an integer.

Finally, Fig. 4 plots the sheath edge as identified in section 2.2. The difference in normalized sheath thickness at the grounded left electrode (S_L) and the powered right electrode (1-S_R) shows an expected 2π periodicity between the points of extremum sheath locations with a

phase lag of π radian for the left electrode. An approximate relation for left and right side normalized sheath thickness can be estimated as $S \approx 0.04 \pm 0.03 \sin 2\pi ft$ with an error of $\sim$4%.

In summary, we developed a two-fluid algorithm for predicting RF discharges and successfully demonstrated its implementation into the MIG code. Results for the charge distributions, current, and sheath details have been documented. In the future, the model will be extended for analyzing two-dimensional RF plasma discharge.

References

[1] Godyak V, Sternberg N. Dynamic model of the electrode sheaths in symmetrically driven RF discharges. Physical Review A 1990;42(4):2299–2312.

[2] Nitschke TE, Graves DB. A comparison of particle-in-cell and fluid model simulations of low pressure radio frequency discharges. J of Applied Physics 1994; 76(10):5646–5660.

[3] Boeuf JP, Pitchford LC. Two-dimensional model of a capacitively coupled RF discharge and comparisons with experiments in the Gaseous Electronics Conference reference reactor. Physical Review E 1995;51(2):1376–1390.

[4] Roy S, Pandey BP, Poggie J, Gaitonde D. Modeling low pressure collisional plasma sheath with space-charge effect. Physics of Plasmas 2003;10(6):2578–2585.

[5] Roy S, Gaitonde D. Radio frequency induced ionized collisional flow model for application at atmospheric pressures. J of Applied Physics 2004;96(5):2476–2481.

[6] Roy S, Pandey BP. Development of a finite element based Hall thruster model. J of Propulsion and Power 2003;19(5):964–971.